

DEUTSCHES ELEKTRONEN-SYNCHROTRON **DESY**

DESY 88-133
September 1988



THE HIGGS MECHANISM IN THE FRAMEWORK OF
LATTICE GAUGE THEORIES

by

H.G. Evertz, M. Marcu

II. Institut f. Theoretische Physik, Universität Hamburg

ISSN 0418-9833

NOTKESTRASSE 85 · 2 HAMBURG 52

DESY behält sich alle Rechte für den Fall der Schutzrechtserteilung und für die wirtschaftliche Verwertung der in diesem Bericht enthaltenen Informationen vor.

DESY reserves all rights for commercial use of information included in this report, especially in case of filing application for or grant of patents.

**To be sure that your preprints are promptly included in the
HIGH ENERGY PHYSICS INDEX ,
send them to the following address (if possible by air mail) :**

**DESY
Bibliothek
Notkestrasse 85
2 Hamburg 52
Germany**

THE HIGGS MECHANISM IN THE FRAMEWORK OF LATTICE GAUGE THEORIES*

Hans Gerd Evertz and Mihail Marcu

II. Institut für Theoretische Physik, Universität Hamburg
Luruper Chaussee 149, D-2000 Hamburg 50, FRG

ABSTRACT

We review the lattice approach to gauge theories with scalar matter fields. Special emphasis is placed on the treatment of the Higgs mechanism in a gauge invariant way. We discuss the strategy for investigating nonperturbatively (e.g. through simulations) the triviality problem and the related problem of upper bounds on the Higgs mass.

1 INTRODUCTION

Lattice gauge theories were introduced by Wilson [1] in order to explain quark confinement in QCD. He defined a gauge invariant regularization in which the theory can be investigated by nonperturbative methods, many of them borrowed from statistical mechanics. Qualitatively this approach is very successful: confinement is explained using strong coupling expansions [1,2,3,4]; the results are extrapolated towards the physically relevant weak coupling region using computer simulations [5]. From a quantitative point of view however, the initial hope of computing hadron masses accurately has not been fulfilled due to the lack of a sufficiently efficient fermion simulation algorithm [6]. While a 10% accuracy is attainable today using quenched fermions (NB: not for the pion) [7], pessimists (optimists) estimate that we need 10^{20} (10^8) times faster computers to go down to a 1% accuracy [8].

For gauge theories coupled to scalar matter fields, present-day computers are powerful enough to allow us to perform accurate simulations [9,10,11]. Of particular interest are the scalar sectors of the standard model and of grand unified theories. In such models perturbation theory is extremely successful; if the “unbroken group” is Abelian (so there is no confinement) it correctly describes the

*Invited lecture presented by M. Marcu at the 12th Johns Hopkins Workshop on Current Problems in Particle Theory, *TeV Physics*, Baltimore, June 8-10 1988.

long distance physics too. Why then would someone want to study such theories on the lattice? Let us discuss several reasons.

First recall Elitzur's theorem stating that a local gauge symmetry cannot be broken [12]. The proof requires the assumption of no gauge fixing. In perturbation theory however we have to fix a gauge, so it is not very clear how to discuss the validity of this theorem. Furthermore, standard descriptions of the Higgs mechanism often give the impression that the local gauge symmetry is in fact broken [13]. We would like to have a gauge invariant formulation of the Higgs mechanism that is explicitly in no conflict with Elitzur's theorem.

Secondly, even in a Higgs mechanism region of a gauge-scalar model perturbation theory does have its problems. Using the renormalization group, we can see that in many cases the cutoff can be removed only for zero renormalized couplings [14,15]. We are either left with a noninteracting – i.e. *trivial* – theory, or we have to keep the cutoff finite and take the point of view that we are dealing with an effective theory. In the latter case upper bounds on the mass of the heaviest Higgs particle can be derived by requiring that it is not heavier than the cutoff. The whole discussion of triviality relies on the renormalization group equations. These equations are expected to hold only for small enough renormalized couplings. It is not clear that this is always true in physically interesting situations, for example if the mass of some Higgs particle is large [16]. Computer simulations can be used to first determine the renormalized couplings nonperturbatively and then to check the validity of the renormalization group equations. They can also be used to check on perturbative predictions considered somewhat less reliable, like the order of the phase transition from the “broken” to the “unbroken” phase [17].

Finally, in the lattice regularization the existence of the quantities we are interested in is guaranteed [3]. We thus have a framework in which more fundamental field-theoretical questions can be investigated, like “in what sense is perturbation theory a good approximation?”. Such questions are not always academic. It is known for example that perturbation theory does not feel the influence of the gauge group center, which is believed to be related to a variety of interesting phenomena [18,19].

We will not attempt here to present a comprehensive review like [10,11]. Our intention will rather be to emphasize the philosophy behind the various numerical lattice investigations, to discuss both their strengths and their weaknesses.

In section 2 we define the lattice regularization and describe the *phase diagrams* for various models. Then we proceed in section 3 to the gauge invariant definition of some important quantities. The *masses* of the gauge bosons and Higgs scalars are determined from the decay of Euclidean correlations. The *renormalized gauge coupling* is extracted from the potential between two static sources. The “Higgs expectation value” is determined from the *vacuum overlap order parameter* [20]. To illustrate typical problems encountered in numerical investigations, we dis-

cuss some examples picked out from various simulations in which these quantities have been measured. We also give an example of an inherently nonperturbative phenomenon on the lattice [19].

In section 4 we discuss the approach to continuum physics using the concept of *lines of constant physics* [21]. In this framework it is easy to understand the problem of triviality. Then we review some of the calculations of an upper bound on the Higgs mass in the $SU(2)$ model with a fundamental scalar field. The best upper bound estimates are actually from studies of the $O(4)$ -symmetric pure matter theory, with the gauge coupling treated perturbatively [22,23,24]. The results of these studies are in very good agreement with the analytic calculations of Lüscher and Weisz for the pure ϕ^4 models [25], which we briefly outline.

In section 5 we give a brief outlook on topics not covered here.

2 LATTICE REGULARIZATION, PHASE DIAGRAMS

In this section we define the lattice regularization for gauge theories with scalar matter fields. In principle, the original model is recovered in the continuum limit, which can be taken in the neighbourhood of second order phase transitions of the lattice model. Therefore the first step in any lattice calculation is the determination of the phase diagram. We discuss several examples of such phase diagrams and the methods employed to obtain them.

2.1 Lattice Regularization and Continuum Limit

The models we are interested in are described by the Euclidean action

$$S_c = \int d^4x \left\{ \frac{1}{2} \text{Tr} F_{\mu\nu}^c F_{\mu\nu}^c + \frac{r}{2} (D_\mu \phi^c, D_\mu \phi^c) + \frac{r}{2} m_c^2 (\phi^c, \phi^c) + \frac{r^2}{4} \lambda_c (\phi^c, \phi^c)^2 \right\} \quad (1)$$

where the sub/superscript c means “continuum”, and the value of r is 1 for a real and 2 for a complex Higgs field ϕ^c . For the gauge group $G=U(1)$, $\frac{1}{2} \text{Tr}$ is replaced by $\frac{1}{4}$. In many cases more than one invariant can be constructed out of the scalar field at one point, and the ϕ^4 potential is more complicated; for simplicity we will not discuss such cases here. We now replace the Euclidean space-time \mathbf{R}^4 with a hypercubic lattice \mathbf{Z}^4 . The lattice gauge field U is a function defined on the set of links $\{x, \mu \mid x \in \mathbf{Z}^4, \mu = 0, 1, 2, 3\}$ that takes its values in the fundamental representation of G . The lattice scalar field ϕ is defined on the lattice sites and takes its values in the representation space of the representation R^ϕ of G . The symbol (\cdot, \cdot) denotes the scalar product in this space. Usually the continuum bare couplings g , m_c and λ_c are replaced by the (positive) lattice bare couplings β , κ and λ :

$$g^2 = \frac{2n}{\beta}; \quad \lambda_c = \frac{\lambda}{\kappa^2}; \quad m_c^2 = \frac{1 - 2\lambda - 8\kappa}{\kappa a^2} \quad (2)$$

where n is the dimension of the fundamental representation of G and a is the lattice spacing. For $G = U(1)$, $2n$ is replaced by 1. The relation between the continuum and the lattice fields is:

$$U_{x,\mu} = \exp\{iagA_{x,\mu}^c\}; \quad \phi_x = \left(\frac{r}{2\kappa}\right)^{\frac{1}{2}} a\phi_x^c \quad (3)$$

κ is called the *hopping parameter* and its meaning is clarified by considering the pure matter theory ($g=0$) at small values of λ_c , where we expect tree-level relations to hold:

- in the unbroken phase, a large and positive m_c^2 , $(am_c)^2 \rightarrow \infty$, corresponds to small κ , and $\kappa \approx (am_c)^{-2} \rightarrow 0$;
- in the broken phase, a large and negative m_c^2 , $(am_c)^2 \rightarrow -\infty$, corresponds to large κ , and $\kappa \approx \frac{r}{2} a^2 \langle \phi^c \rangle^2 \approx -(am_c)^2 / 2\lambda_c$;
- the phase transition is at $m_c \approx 0$, which corresponds to $\kappa \approx \frac{1}{8}$.

(for large λ it turns out that small κ still corresponds to the unbroken and large κ to the broken phase). The lattice action is

$$S = \beta \sum_p \left\{ 1 - \frac{1}{2n} \text{Tr} [U(p) + U^\dagger(p)] \right\} - \kappa \sum_{x,\mu} 2 \text{Re} (\phi_x, R^\mu(U_{x,\mu})\phi_{x+\hat{\mu}}) \\ + \lambda \sum_x [(\phi_x, \phi_x) - 1]^2 + \sum_x (\phi_x, \phi_x) \quad (4)$$

where $U(p)$ is the path ordered product of the gauge fields around the elementary plaquette p . Formally $S \rightarrow S_c$ in the limit $a \rightarrow 0$.

The lattice spacing a does not occur at all in (4). The formal limit $a \rightarrow 0$ is meaningless unless we define a within the lattice theory itself. This can be achieved by identifying a^{-1} with the ultraviolet cutoff. Let ξ_1 be a correlation length in lattice units (i.e. a real number). We define a as the dimensionful quantity for which $a\xi_1 = \xi_1^c$, where ξ_1^c is a physical length that we fix by hand, e.g. by requiring it to be equal to the inverse of some particle mass. The continuum limit $a \rightarrow 0$ can be taken only if $\xi_1(g, \kappa, \lambda) \rightarrow \infty$, that is by tuning the couplings towards a *second order phase transition* point $(g_{cr}, \kappa_{cr}, \lambda_{cr})$ where ξ_1 is infinite.

In the case of the pure gauge theory ($\kappa=0$) with a nonabelian G , we expect from asymptotic freedom that the correlation lengths become infinite in lattice units at $g=0$ [1,5]. The continuum limit is performed by checking that for $g \rightarrow 0$ the lattice theory obeys *scaling laws*:

$$\frac{\xi_i}{\xi_1} \approx \frac{\xi_i^c}{\xi_1^c} = \text{const} \quad (5)$$

where ξ_i are other correlation lengths in lattice units and ξ_i^c ($i \neq 1$) are the corresponding continuum quantities with the dimension of length. For dimensionless physical quantities scaling simply means that they are constant for small enough g . If in addition to scaling $\xi_1(g)$ coincides with the prediction of the renormalization group improved perturbation theory, we say that *asymptotic scaling* is obeyed [5].

For the full theory the situation is more complicated since the values of the ratios (5) depend in general on the path on which $(g_{cr}, \kappa_{cr}, \lambda_{cr})$ is approached. A useful procedure [21] is to define *lines of constant physics* as lines on which two of the ratios (5) have fixed values (one can equivalently fix dimensionless physical quantities). The continuum limit is taken by checking scaling along a line of constant physics.

In QCD with fermions (3 flavors, $m_u = m_d$), a useful definition of the lines of constant physics is to fix the ratios of the rho mass to the pion mass and to the kaon mass. Scaling then means to check that the other hadron masses are constant as the critical point is approached. In section 4 we will see that for gauge-Higgs systems a useful definition is to fix the ratio of the Higgs to the W mass and the value of the renormalized gauge coupling.

2.2 Computational Methods on the Lattice and Phase Diagrams

Since the whole theory is in general rather complicated, it is a good idea to start investigating the phase diagram in some limiting cases. Two limits are straightforward. For $\beta \rightarrow \infty$ ($g \rightarrow 0$) the gauge interaction vanishes and we get the pure ϕ^4 matter theory. For $\kappa \rightarrow 0$ the mass term for the ϕ -field becomes infinite and we get the pure gauge theory.

As $\beta \rightarrow 0$ the gauge fields occur only in the link term of the action (4) and can be integrated out exactly. The result is a pure matter theory whose variables are the G-invariant polynomials in ϕ_x (often only functions of (ϕ_x, ϕ_x) [26]).

If we let $\lambda \rightarrow \infty$ (so ϕ has length one) and then $\kappa \rightarrow \infty$, the link term in (4) is bounded and must be as large as possible. In the unitary gauge ϕ takes its values in a set of orbit representatives [27]. The link term is maximal if ϕ_x is the same orbit representative Φ for all x and $U_{x,\mu}$ is in its stability group H_Φ . The largest stability group H_{max} wins by an entropy factor for each link, so we are left with a pure gauge theory with the gauge group H_{max} .

There are a variety of computational tools that can be used in the study of the lattice regularized theories, some of them similar to those in continuum field theory, others adapted from statistical mechanics. Among the most important are:

- Convergent expansions [1,2,3,4] can be set up in the full theory for small β (strong coupling), and in the pure matter theory for small κ .
- Expansions around one of the limiting theories have been used in several

contexts: the hopping parameter expansion [28] is an expansion in κ around the pure gauge theory; the weak gauge coupling expansion is an expansion in g^2 around the pure matter theory [29,21].

- Computer (Monte Carlo) simulations [5,9] can be used in the whole phase diagram except in regions with large correlation lengths (presently 5 begins to be large, 10 is huge). They are especially useful in investigating the location and order of the phase transitions and the critical behaviour.
- Perturbative expansions can be used on the lattice as well as in the continuum [5,30]. The perturbative expressions for the beta functions are widely used to predict the critical behaviour (see e.g. [5,31,25]).

Other methods include mean field, large N , spin waves, variational and expansion methods for the Hamiltonian.

Let us now turn to the discussion of some typical phase diagrams. For simplicity choose $G = U(1)$, $SU(2)$, and $SU(3)$. The scalar field has charge 1 or 2 in the $U(1)$ case, and is in the fundamental or in the adjoint representation in the nonabelian cases.

Fig. 1 depicts the phase diagrams for $\lambda = \infty$ [2,32,4,10]. In general there are three distinct regions: the Coulomb phase (scalar electrodynamics), the Higgs mechanism region and the confinement region. The Coulomb phase exists only for the $U(1)$ models; it has to be a separate phase since it has a massless photon, while for these models all asymptotic particles are massive both in the confinement and in the Higgs region. For continuous nonabelian gauge groups, no examples of theories with a Coulomb phase are known. It is widely believed that gauge invariant charged states carrying a nonabelian charge cannot exist.

A lot is known about the limiting theories. For $\beta \rightarrow \infty$ the $O(N)$ spin system (N is the real dimension of the Higgs field representation) always has a second order phase transition [31]. For $\kappa \rightarrow 0$ the pure gauge theory has a phase transition in the $U(1)$ case [33], but not in the $SU(2)$ and $SU(3)$ cases [5]. The order of the $U(1)$ transition is very difficult to determine [34]. For $\kappa \rightarrow \infty$ one gets other pure gauge theories, as discussed below. At $\lambda = \infty$ and $\beta = 0$ the theory becomes noninteracting and does not have a phase transition.

If the scalar field is in the *fundamental representation* (charge-1 for $U(1)$), the Higgs mechanism and the confinement regions are *analytically connected* (i.e. in the same phase). This remarkable result was proven for the $U(1)$ and the $SU(2)$ cases [2,3]. In these cases the theory becomes noninteracting in the limit $\lambda = \infty$, $\kappa \rightarrow \infty$, and the small- β expansion can be analytically continued to the large- β , large- κ corner. In figs. 1a and 1c we hatched the whole convergent expansion region obtained in this way. For $G = SU(3)$, the convergent expansion region is smaller, resembling to the one depicted in fig. 1d. The reason is that for $\lambda = \infty$,

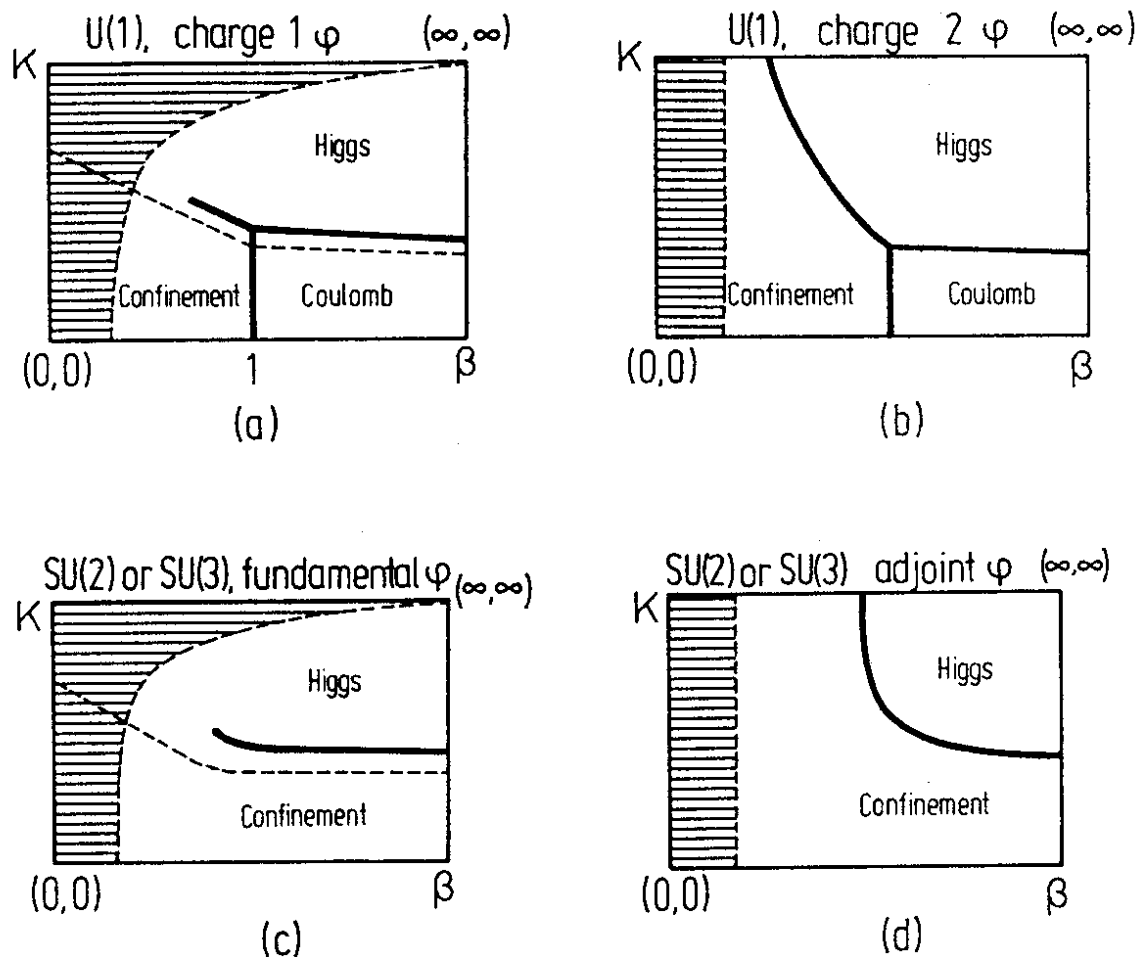


Figure 1: Phase diagrams at $\lambda = \infty$. The solid lines are the phase boundaries. In the hatched regions convergent expansions exist (with a modification for the $SU(3)$ model with a fundamental scalar field – see text). The dashed lines show schematically how the transition lines change for small λ .

$\kappa \rightarrow \infty$ the model becomes an $SU(2)$ pure gauge theory, so unlike the case of a noninteracting limit the small- β expansion has to break down at a finite value of β . Nevertheless, since the $SU(2)$ pure gauge theory does not have a phase transition, the phase diagram of the $SU(3)$ model with a fundamental scalar field is similar to that of the $SU(2)$ model.

In the confinement region, the force between a fundamental static source-antisource pair can only be screened by a dynamical matter field in the fundamental representation (otherwise the string between the source-antisource cannot break). In the Higgs mechanism region on the other hand, the vacuum is similar to a plasma of charged matter particles and screening is always possible. Thus if the scalar field is in the *adjoint representation*, or if it has charge 2 in the $U(1)$

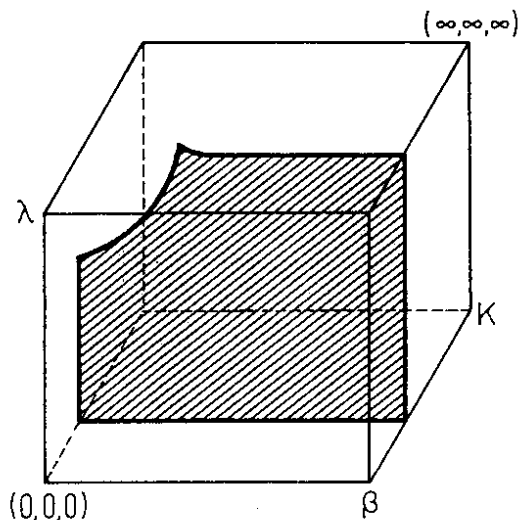


Figure 2: Schematic three parameter phase diagram for the $SU(2)$ or $SU(3)$ lattice gauge theory with a fundamental scalar matter field.

case, there has to be a *confinement-Higgs phase transition* [32]. For $\lambda = \infty$, $\kappa \rightarrow \infty$ this transition goes over into the transition of the Z_2 pure gauge theory for the charge-2 $U(1)$ case (fig. 1b), and into that of the $U(1)$ and $U(2)$ pure gauge theories for the $SU(2)$ -adjoint and $SU(3)$ -adjoint cases respectively (fig. 1d). The Z_2 pure gauge theory has a first order phase transition [35]. The $U(2)$ theory has a transition coming from its $U(1)$ part. In fig. 1d all particles are massive in the confinement phase, but in the Higgs phase there is a massless “photon”.

As λ decreases the phase transitions shift. In figs. 1a and 1c, the dashed lines depict the change in the transition lines. For small enough λ the Higgs-confinement transition extends up to $\beta = 0$ [10,26]. In fig. 2 the whole phase diagram of the $SU(2)$ or $SU(3)$ model with a fundamental scalar field is drawn. There is only one phase throughout, because of the hole in the transition surface at large λ .

At large β , the Higgs-Coulomb transition for $U(1)$ and the Higgs-confinement transition for the other cases are expected to be *first order* by the standard Coleman-Weinberg argument concerning radiative corrections [17]. As will be seen in section 4, this is a very important point in the discussion of the triviality problem. For part of the transition surface, simulations have confirmed this expectation. As an example for such a calculation, in fig. 3 some results from [36] are presented. The expectation value of the link term in the action (4) is plotted for the $SU(2)$ model with a fundamental scalar at $\lambda = 0.5$ and $\beta = 2.25$. The jump at some value κ_{cr} of κ indicates a first order transition. Another sign for the first order transition is the two-state signal seen in the histogram at $\kappa = 0.2706$ (also for the link term). The jump at $\kappa_{cr}(\beta, \lambda)$ was found to become smaller as β increases. This had been expected, since at $\beta = \infty$ the transition is second order

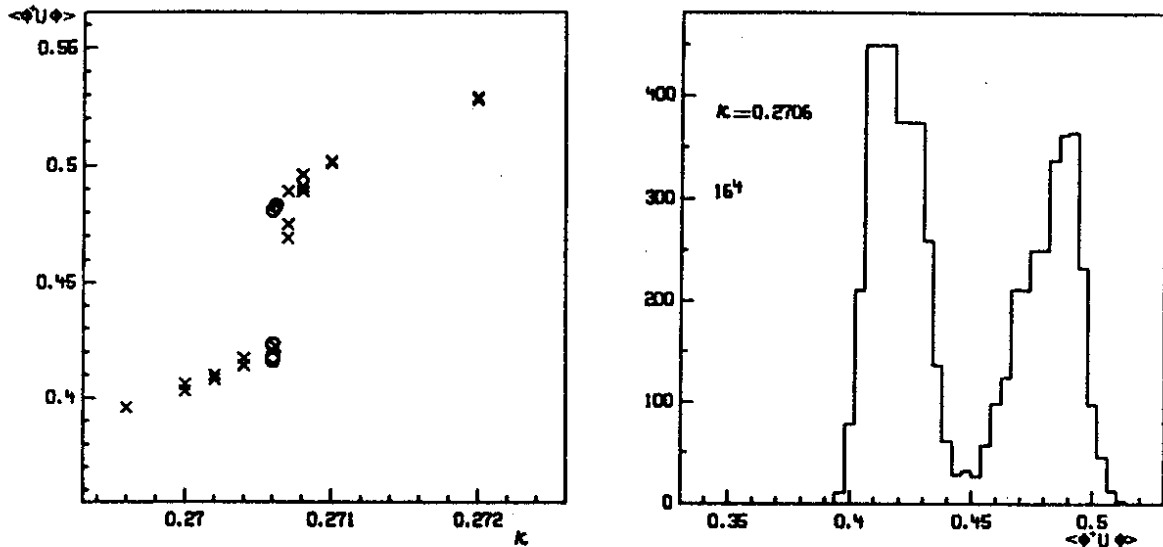


Figure 3: Numerical investigation of the Higgs-confinement transition for the $SU(2)$ model with a fundamental scalar field at $\lambda=0.5$ and $\beta=2.25$ on a 16^4 lattice (from [36]).

(with both the vector boson and the Higgs scalar mass becoming zero in lattice units). The jump also becomes smaller as β decreases towards the other endpoint of the fixed- λ transition line, which is expected to be second order too [26]. The exact location of the small- β endpoint is however very difficult to find numerically.

One should be very careful with the statement that the simulation results confirm the Coleman-Weinberg prediction of a first order transition. The region investigated in simulations is rather limited. In general, it is impossible to distinguish numerically between a weakly first order transition and a second order transition. If the correlation length is not small compared to the lattice size, weird things may happen: one can get a two-state signal although the transition is in fact second order, or one can get scaling laws indicating a second order transition although the transition is in fact first order. For large β , where some correlation length is always large, the lattice size limitations inherent to any simulation make a numerical investigation of the transition impossible.

The Coleman-Weinberg argument [17] uses the assumption that λ_{ren} and g_{ren}^4 are of the same order of magnitude (“ren” means renormalized). This assumption is supported by a conventional analysis of the renormalization group flow (see e.g. [15]). It is not clear that it is true near the whole transition surface. An argument was proposed by Nill [37] to the effect that the phase transition surface has two distinct regions separated by a tricritical line, as shown in fig. 4. In one region $\lambda_{ren} \sim g_{ren}^4$ and the Coleman-Weinberg arguments apply. In the second region λ_{ren} is much larger than g_{ren}^4 and the transition (Higgs-Coulomb for $U(1)$, Higgs-confinement for $SU(2)$) is second order. At constant λ this second region is the

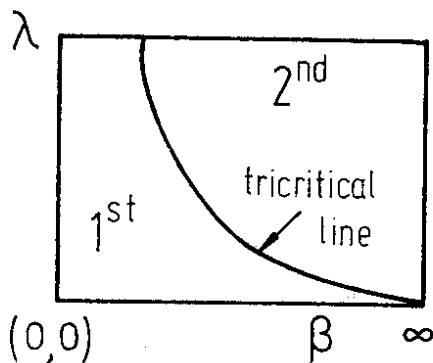


Figure 4: Nill's conjecture for the phase transition surface.

large- β region of the transition surface. In view of Nill's argument it would be interesting to put more effort into the numerical study of this phase transition.

3 GAUGE INVARIANT DISCUSSION OF THE HIGGS MECHANISM ON THE LATTICE

Elitzur's theorem [12] tells us that in a description of the theory that does not require gauge fixing, the local gauge symmetry is not broken. If one wishes to use perturbation theory however (and there obviously are good reasons for that), gauge fixing is a necessity. The quantities easiest accessible to computations are then vacuum expectation values of non-gauge-invariant operators like n -point-functions (of simple expressions in the fields that occur in the Lagrangian). There is always a unique gauge invariant quantity having the same vacuum expectation value as a given non-gauge-invariant one, but it is in most cases highly nonlocal and we are neither able to compute it explicitly nor to understand it beyond rough properties like e.g. the connection between some of the poles in the n -point-functions and particle masses. One important exception is of course the S -matrix, which does not depend on the gauge choice [13]. On the other hand the Higgs mechanism is usually discussed using a gauge dependent effective potential [17].

If we want to describe the Higgs mechanism in a gauge invariant way, there is a price to pay: the perturbative computation of the relevant quantities will be considerably more complicated. As a reward there should be a gain in physical understanding. One gauge invariant description was extensively discussed in this conference, namely the effective action of Vilkoviskii and de Witt [38]. In that approach however, the problem of not knowing the exact physical meaning of the n -point-functions still persists. Here we shall take the point of view that the only way to understand the meaning of nonlocal quantities is to define them as limits of well-understood local gauge invariant quantities.

Using the lattice regularization will help us in many ways. First, we are guaranteed that the expectation values of local quantities exist (this is obvious

on a finite lattice; then one shows that the thermodynamical limit exists [3]). We can use the reconstruction theorem for Euclidean field theories [39,2] in order to understand these quantities in terms of a quantum mechanics in a separable Hilbert space. Secondly, as discussed in section 2, we can use nonperturbative methods and attempt not only to understand the Higgs mechanism in a gauge invariant way, but also to check the validity of perturbative results.

In this section we discuss some of the most important quantities used in the study of Higgs regions of lattice gauge theories with scalar matter fields: masses, renormalized gauge coupling, and Higgs expectation value. We describe as examples some results of Monte Carlo simulations.

Simulations cannot be used for really large correlation lengths. Perturbation theory on the other hand works best at small gauge couplings, which almost always means large correlation lengths (and which often is the region of physical interest). If we are lucky, the region where simulations do not require a prohibitive amount of computer time overlaps with the region where perturbation theory holds to an order that can still be computed. Agreement between simulations and perturbation theory is then a stringent test for the latter, since it is not done in the region where it works best (i.e. at really large correlation lengths). It has to be mentioned that a perturbative calculation beyond the leading order has not been performed for all gauge invariant quantities accessible to simulations that we are going to describe.

The success of the standard model suggests that using perturbation theory is in fact legal for most purposes. We cannot however take this for granted, since only a limited energy range has been explored by experiments and since the Higgs particle is still a puzzle. In the lattice framework we can look for nonperturbative phenomena. It is not hard to find candidates, since perturbation theory only takes into account small fluctuations around a Gaussian fixed point. At the end of this section we briefly discuss some relatively stable excitations that exist on the lattice but cannot be described perturbatively. Nothing is known however about their relevance to continuum physics.

3.1 Masses

One of the main predictions of the Higgs mechanism concerns the particle states of the theory. They are not in a naïve one-to-one relation with the fields in the Lagrangian. We have stable massive spin one particles, which we shall generically call the “ W ”, spin zero particles with vacuum quantum numbers which we shall call “Higgs”, and, depending on the model considered, massless “photons”.

On the lattice, the standard way to compute masses is from the decay of two-point-functions in Euclidean time. We shall discuss here only the simplest case of particles that have trivial quantum numbers with respect to the “unbroken group”. In this case we can couple to the particle states using gauge invariant

operators.

Let $\mathcal{O}(\underline{x})$ be a local gauge invariant time-zero operator (the underlined symbols denote objects in the time-zero hyperplane), define its Fourier transform by

$$\mathcal{O}(\underline{q}) = \sum_{\underline{x}} \mathcal{O}(\underline{x}) e^{i\underline{q}\underline{x}} \quad (6)$$

and denote by $E(\underline{q})$ the momentum dependent energy of the lightest one-particle state $1_{\underline{q}}$ to which $\mathcal{O}(\underline{x})$ couples. $E(\underline{q})$ is then determined by the leading behaviour for large Euclidean times t of the correlation (H is the Hamiltonian):

$$\langle 0 | \mathcal{O}^\dagger(\underline{q}) e^{-tH} \mathcal{O}(\underline{q}) | 0 \rangle - |\langle 0 | \mathcal{O}(\underline{q}) | 0 \rangle|^2 \approx |\langle 0 | \mathcal{O}(\underline{q}) | 1_{\underline{q}} \rangle|^2 e^{-tE(\underline{q})} \quad (7)$$

In simulations, periodic boundary conditions (which are almost always used) and the finiteness of the time direction force us to replace the exponential decay by a periodic exponential,

$$e^{-tE(\underline{q})} \rightarrow \left(e^{-tE(\underline{q})} + e^{-(L_t - t)E(\underline{q})} \right) \quad (8)$$

since a particle can be exchanged between the zero and t hyperplanes either directly or around the torus (L_t is the number of lattice sites in time direction). $E(\underline{q})$ is then determined by fitting the data from a Monte Carlo simulation with the form (7-8) [40]-[45]. Usually the small values of t , $t < t_{min}$, have to be disregarded, since there the contribution of higher excited states is not negligible.

This procedure is on shakier theoretical grounds if we deal with a resonance rather than a stable particle. Since the Higgs is a resonance if it is heavier than twice the W , this is an important situation. For a narrow resonance, the r.h.s. of (7) can be approximated by:

$$|\langle 0 | \mathcal{O}(\underline{q}) | 1_{\underline{q}}^{res} \rangle|^2 e^{-tE_1^{res}(\underline{q})} + \sum_{2_{\underline{q}}^{stable}} |\langle 0 | \mathcal{O}(\underline{q}) | 2_{\underline{q}}^{stable} \rangle|^2 e^{-tE_2^{stable}(\underline{q})} \quad (9)$$

where 1 and the superscript *res* denote a one-resonance state, while 2 and *stable* denote a state containing two stable particles. The sum is over the various two-particle states with total momentum \underline{q} . If $E_2^{stable}(\underline{q}) < E_1^{res}(\underline{q})$, the second term always dominates for t large enough. On the other hand, the *local* operator $\mathcal{O}(\underline{x})$ couples much stronger to a one-resonance state than to the more delocalized two-stable-particle states, so for small t the first term dominates because of the matrix elements in front of the exponentials. In most numerical investigations a range $t_{min} < t < t_{max}$ was found for which the mass of the Higgs resonance could be determined from a clean exponential decay with $E_1^{res}(\underline{q})$.

Let us discuss the choice of $\mathcal{O}(\underline{x})$ in the $SU(2)$ model with a fundamental scalar field [40]-[43],[36]. Denote by ρ_x the square root of (ϕ_x, ϕ_x) , by $\sigma(\phi)$ the

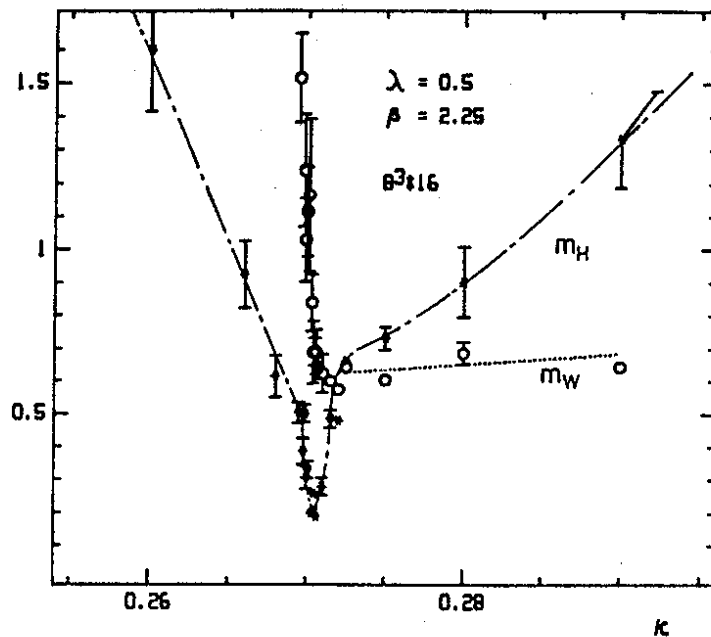


Figure 5: Masses of the Higgs and W particles for the $SU(2)$ model with a fundamental scalar field at $\lambda=0.5$ and $\beta=2.25$ on an $8^3 \times 16$ lattice (from [40,36]). The lines are drawn to guide the eye.

unitary matrix that is determined uniquely from the equation $\phi = \rho \sigma(\phi) \begin{pmatrix} 1 \\ 0 \end{pmatrix}$, and by τ_b the Pauli matrices ($b=1, 2, 3$). We introduce the new link variables $W_{x,\mu} = \sigma(\phi_x)^\dagger U_{x,\mu} \sigma(\phi_{x+\hat{\mu}})$. The model has a global $SU(2)$ “isospin” symmetry, namely the conjugation of the $W_{x,\mu}$ with a constant 2×2 matrix. To measure the W mass, we can take $\mathcal{O}(\underline{x}) = \text{Tr } \tau_b W_{\underline{x},j}$ (j denotes the spatial directions). This is a 1^{--} isospin-1 operator. For the Higgs mass we can use the 0^{++} isospin-0 operators $\mathcal{O}(\underline{x}) = \rho_{\underline{x}}^2$ or $\mathcal{O}(\underline{x}) = \sum_j \text{Tr } W_{\underline{x},j}$. In the confinement phase the same operators couple “bosonium” states (bound states of two scalar quarks) with the corresponding quantum numbers.

We have denoted here with the same symbol two entirely different objects: the classical fields and the time-zero field operators. This should not cause any ambiguities, since the former occur in the context of Euclidean path-integral expectation values, while the latter are used in quantum-mechanical matrix elements.

In fig. 5 the W and Higgs masses are shown for a typical situation [40,36], at $\lambda=0.5$ and $\beta=2.25$ (cf. fig. 3) As $\kappa \rightarrow 0$ the bosonium states become infinitely heavy. This explains the sharp rise in both masses as κ decreases below the phase transition. Above the transition, the W mass increases slowly with κ . Close to the transition it is almost constant, but for larger κ standard tree-level relations say it has to be linear in κ . The Higgs mass increases much more steeply with κ . It is relatively small only in a narrow region around κ_{cr} . If the transition were second order, the Higgs mass would become zero at κ_{cr} (on an infinite lattice).

In order to give some insight into the problems encountered in the understanding of simulation results, let us discuss the pronounced dip in the Higgs mass that in our example occurs in the region around the phase transition. This dip was not seen at large λ [41,43]. As β increases, it becomes more shallow [40]. It is not clear what causes this phenomenon. It may be a real effect in the sense that it persists for large β (and has been observed only in a small β -region because of problems with simulations at large correlation lengths). On the other hand it may be a spurious effect from the point of view of continuum physics. One possibility is that the dip is due to the proximity of the small- β end of the transition line, where we expect that only the Higgs mass becomes zero in lattice units [26]. A second possibility is that it is caused by the fact that, close to a weak first order transition, the tunneling between the stable and the metastable state produces on small volumes a very small mass gap [46] (actually this mass gap is even smaller on large lattices, but for large enough systems the tunneling probability is so small that no tunneling event happens during the time of the simulation). Finally it is possible that the dip is due to the existence of a very light glueball-like particle with vacuum quantum numbers for κ just below the transition. In this case it would be very hard to do any reliable computations in the confinement phase [43]. Actually there are indications that all three considerations do play a role.

In the $U(1)$ model with a charge one scalar field an operator that couples to the W is $\mathcal{O}(\underline{x}) = \text{Im } \bar{\phi}_{\underline{x}} U_{\underline{x},j} \phi_{\underline{x}+\hat{j}}$ (the bar denotes complex conjugation). For the Higgs particle we can choose $\mathcal{O}(\underline{x}) = \bar{\phi}_{\underline{x}} \phi_{\underline{x}}$ or $\mathcal{O}(\underline{x}) = \sum_j \text{Re } \bar{\phi}_{\underline{x}} U_{\underline{x},j} \phi_{\underline{x}+\hat{j}}$. In the Coulomb phase these operators couple to scalar-electron positronium states with the appropriate quantum numbers. The masses measured with these operators have been found to behave in κ in a way similar to the $SU(2)$ case [44] (the Higgs phases are similar anyway; for the bosonium bound states we expect no dramatic difference between the confinement phase of the $SU(2)$ model and the Coulomb phase of the $U(1)$ model).

In the Coulomb phase there is a massless photon. One example of a gauge invariant operator to which it couples is the B -field, $\mathcal{O}(\underline{x}) = \text{Im } U(\underline{p})$, where \underline{x} is a corner of the spatial plaquette \underline{p} . For zero momentum, we do not expect any signal in the Euclidean correlation (7) since a photon at rest should not exist. For finite momenta however this is no longer true and we expect $E(\underline{q})$ to obey a lattice dispersion relation [45,44] (for small \underline{q} , $E(\underline{q}) \approx |\underline{q}|$ as in the continuum, but for a typical lattice size used in simulations even the smallest nonzero momenta are too large for the lattice corrections to be negligible). It is reassuring that these theoretical expectations were fully confirmed by simulation results [44]. One can even do more sophisticated things like projecting out photons with a given helicity [45]. In the Higgs phase there should be no photon and, at nonzero momenta, $\text{Im } U(\underline{p})$ should couple to the massive W (at zero momentum this is not true because of parity; there is no coupling to the Higgs because of charge conjugation).

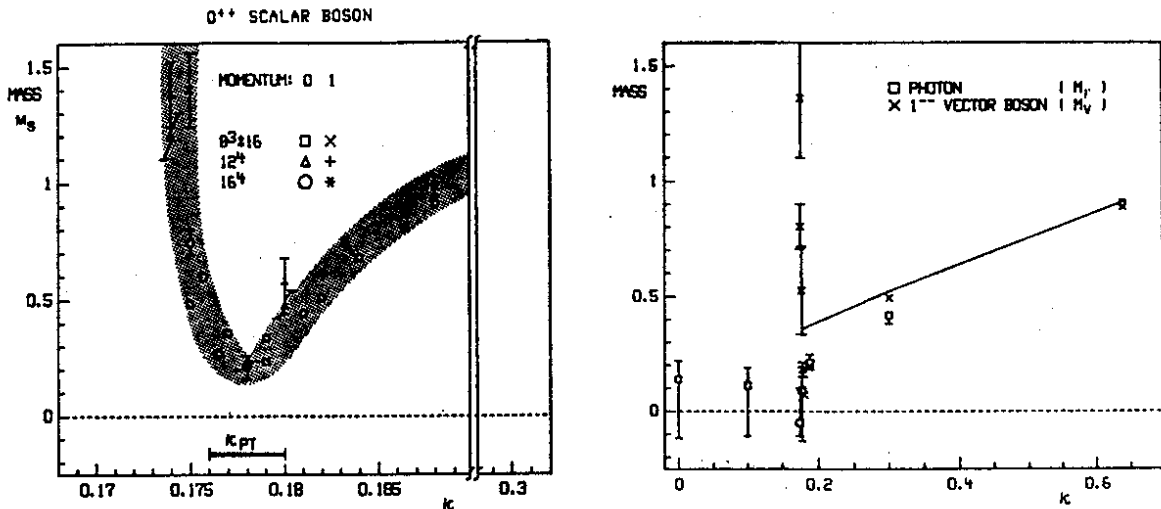


Figure 6: Masses in the $U(1)$ model with a charge-1 scalar field at $\lambda=3.0$ and $\beta=2.5$ on an $8^3 \times 16$ lattice (from [44]). The lines are drawn to guide the eye. Notice the different ranges for κ in the two plots.

The simulation results from [44] shown in fig. 6 confirm this expectation too.

3.2 Renormalized Gauge Coupling

In lattice theories, scattering processes can be described within a rigorous framework [47]. It is not practical however to define the renormalized gauge coupling starting from scattering amplitudes, since we are far from being able to compute such quantities on the lattice reliably. Fortunately there is a different way.

Consider a rectangular contour L with sides of length r in one of the space directions and t in Euclidean time. The basic quantity is the Wilson loop $W(r, t)$, which is the Euclidean expectation value of the trace of the path ordered product of the U -fields around L . Its physical meaning is well known [1,5]: it is the expectation value of the Euclidean evolution operator $\exp(-tH)$ in a state containing an external source-antisource pair separated by a spatial distance r .

A source is a state that transforms according to an irreducible representation of the gauge transformation operators at some point \underline{x} . Since the gauge symmetry is exact, this property is preserved in time, and we say that the source does not move. Sources can also be constructed by adding to the theory a second matter field ψ with a very large mass M . In the limit $M \rightarrow \infty$ there is a one-to-one correspondence between the gauge invariant states of the extended theory that contain ψ -particles, and the states in the original theory that contain sources. Thus we arrive at the interpretation that a source is an external particle that does not move because it is infinitely heavy.

In the limit $t \rightarrow \infty$, $\exp(-tH)$ projects out the lowest-energy state in the sector containing the source-antisource pair. This state is an eigenstate of the Hamiltonian. We shall call it a pair of *static* sources, since it no longer changes in time.

For static sources the classical concept of a potential (or force) can be defined. The representation of the source is the same as the representation used for the U -fields in the Wilson loop. For simplicity we shall assume it to be the fundamental representation from now on. The potential $V(r)$ between a source-antisource pair is then obtained from the Wilson loop as follows:

$$V(r) = - \lim_{t \rightarrow \infty} \frac{1}{t} \log W(r, t) \quad (10)$$

In the Higgs region, the first guess for the functional form of $V(r)$ is the Yukawa potential, which is derived in the one- W -exchange approximation [41]:

$$V(r) = -c \frac{\alpha_{ren}}{r} \exp\{-am_W r\} + 2E_q \quad (11)$$

where c is a group theoretical constant (1 for $U(1)$ and $3/4$ for $SU(2)$), α_{ren} is related to the renormalized gauge coupling by the usual relation $\alpha_{ren} = g_{ren}^2/4\pi$, m_W is the W mass as defined in section 3.1, and E_q is the energy of an isolated static source.

In several simulations [41,48,42,43] it was found that (11) was fulfilled within statistical errors by the potentials obtained from the measured Wilson loops using (10). This was not only true for very weak gauge couplings (this case was studied in [42]). In [43] for example, the Yukawa potential fitted the Monte Carlo data well even though α_{ren} was more than 2.5 times larger than α_{bare} . If α_{bare} is increased still further, the one- W -exchange approximation of course breaks down. For a better comparison with the simulation results, corrections to (11) should be computed.

3.3 Higgs Expectation Value

A gauge invariant, gauge independent quantity that can be used as ‘‘Higgs expectation value’’ is the vacuum overlap order parameter (VOOP). This quantity tests the existence of charged states. The ideas leading to the VOOP, its definition and some fundamental properties have been discussed in [20]. Let us summarize the most relevant aspects. We remind that underlining denotes purely spatial (3-dimensional) objects (equivalently: objects in the time-zero hyperplane).

Let $\underline{L}_{\underline{x}\underline{x}'}$ be a spatial path from \underline{x} to \underline{x}' , chosen for simplicity to be a straight line. A naïve candidate for a dynamical charge-anticharge (‘‘dipole’’) state is:

$$\phi^\dagger(\underline{x}) U(\underline{L}_{\underline{x}\underline{x}'}) \phi(\underline{x}') |0\rangle \quad (12)$$

where $U(\underline{L}_{\underline{x}\underline{x}'})$ is the path ordered product of the U -fields along $\underline{L}_{\underline{x}\underline{x}'}$. For large separations the energy of this gauge invariant state is proportional to $|\underline{x} - \underline{x}'|$. It

can be regularized by translating the operator $U(\underline{L}_{\underline{x}\underline{x}'})$ that creates the electric flux from \underline{x}' to \underline{x} by n lattice units into Euclidean time. The following general and model-independent result holds [20]. The energy of the Hilbert space vector (to avoid any confusion concerning ordering problems we write the group indices a and b explicitly this only time)

$$|\underline{x}, \underline{x}', n\rangle := \phi^\dagger(\underline{x})_a \phi(\underline{x}')_b e^{-nH} U_{ab}(\underline{L}_{\underline{x}\underline{x}'}) |0\rangle \quad (13)$$

stays bounded as $|\underline{x} - \underline{x}'| \rightarrow \infty$ provided that for some constant c , $n \geq c|\underline{x} - \underline{x}'|$ (i.e. provided the regulating parameter n grows at least linearly with the distance between \underline{x} and \underline{x}').

Notice that the state translated into Euclidean time is not gauge-invariant. For $n \rightarrow \infty$, e^{-nH} projects out the lowest energy state in the presence of a source-antisource pair. This means not only that the electric field spreads out in such a way as to minimize the energy (think about the Coulomb field of a dipole as an example), but also that other effects, like vacuum polarization, are adequately taken into account. After having regularized the energy, we use the ϕ -operators to replace the sources with dynamical fields. If we would act with e^{-nH} on the gauge invariant state (12), the state projected out would be the vacuum, so there would be no electric flux from \underline{x} to \underline{x}' at all.

In the limit $\underline{x}' \rightarrow \infty$, $n \geq c|\underline{x} - \underline{x}'|$, the charge at \underline{x} either becomes free or is screened. A quantity that distinguishes between the two situations is the vacuum overlap of the normalized dipole state (13):

$$\tilde{\rho}(|\underline{x} - \underline{x}'|, n) := \frac{\langle 0 | \underline{x}, \underline{x}', n \rangle}{\| |\underline{x}, \underline{x}', n \rangle \|} \quad (14)$$

A free charge is orthogonal to the vacuum Hilbert space. If the charge is screened, the dipole state (13) differs from the vacuum only in the neighbourhood of \underline{x} and \underline{x}' . If $\phi(\underline{x})$ has no additional nontrivial quantum numbers, the vacuum overlap is nonzero in the limit. Thus the criterion for existence of charged states is:

$$\tilde{\rho}(\infty, \infty) = \begin{cases} 0 & \exists \text{ free charges} \\ \neq 0 & \text{charges are screened} \end{cases} \quad (15)$$

The vacuum overlap is easily expressed in terms of euclidean expectation values. In order to have a quantity with a similar renormalization as the ϕ -two-point-function (i.e. the usual wave function renormalization), it is convenient to redefine (14) by replacing in the denominator $|\underline{x}, \underline{x}', n\rangle$ with $e^{-nH} U(\underline{L}_{\underline{x}\underline{x}'}) |0\rangle$. Denoting the resulting quantity by ρ instead of $\tilde{\rho}$, we obtain:

$$\rho(|\underline{x} - \underline{x}'|, n) = \frac{\langle \begin{array}{c} \underline{x} \quad \underline{x}' \\ \text{---} \\ \bullet \quad \bullet \\ \text{---} \\ n \end{array} \rangle}{\langle \begin{array}{c} \text{---} \\ \text{---} \\ \text{---} \\ 2n \end{array} \rangle^{\frac{1}{2}}} \quad (16)$$

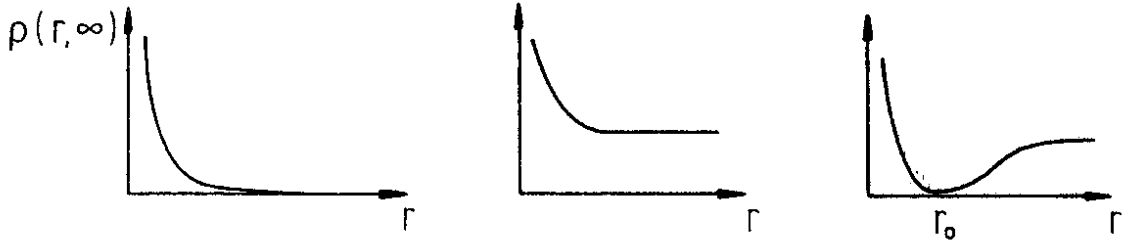


Figure 7: Qualitative behaviour of the gauge invariant ϕ -two-point-function in a free charge phase (left), in a Higgs mechanism region (middle) and in a confinement region (right).

On the r.h.s. we have used a pictorial notation for the Euclidean expectation values of path ordered products of U -fields along space-time paths. The horizontal lines are time translations of the path $\underline{L}_{\underline{x}\underline{x}'}$. The vertical lines are at the location of the sources, and come from the fact that in going from the quantum mechanical to the path integral formulation we go from the temporal gauge to a description without any gauge fixing. The dots represent the ϕ -fields (at time zero).

The criterion (15) also holds for ρ (with ρ a related interpretation is also possible: (15) tests whether the charge of a static source is screened or not). The cancellation of perimeter contributions between the numerator and denominator of (16) is one of the main ingredients in proving (15). The order parameter (the VOOP) is $\rho(\infty, \infty)$.

$\rho(|\underline{x} - \underline{x}'|, \infty)$ is a gauge-invariant two-point function of the ϕ -field. Its dependence on the distance is shown qualitatively in fig. 7. It is relatively easily accessible by numerical methods in a free charge phase and in a Higgs region, where it behaves similarly to the matter field two-point function of the pure matter ($\beta = \infty$) theory. In a confinement region however, $\rho(|\underline{x} - \underline{x}'|, \infty)$ has a free-charge-like decrease with $|\underline{x} - \underline{x}'|$ at small distances (corresponding to the Coulomb plus linear region of the potential), where a charge-anticharge (quark-antiquark) pair can exist as an excitation. At large distances however it goes to a constant (after the potential becomes flat). Thus it should have a dip around the characteristic length for hadronization (fragmentation).

In a Higgs region, the “Higgs expectation value” v is connected to the VOOP by the tree level relation (the lattice constant a is used to produce dimensionless quantities):

$$(av)^2 \simeq \kappa \rho(\infty, \infty) \quad (17)$$

The *renormalized* Higgs expectation value cannot be obtained from the VOOP alone because we would also have to take into account the wave function renormalization for the two endpoints. For this a computation of the VOOP beyond tree level is needed.

From a technical point of view, it is worth noting that in order to obtain

reliable values for $\rho(\infty, \infty)$, the $n \rightarrow \infty$ extrapolation has to be performed first (see [43]) for details).

The VOOB has been used to investigate gauge-Higgs models numerically: Z_2 [49], $U(1)$ -charge-1 [50], $U(1)$ -charge-2 [51], $SU(2)$ -fundamental [48,43] and $SU(2)$ -adjoint [52].

Let us briefly discuss the simulation results [43] for the $SU(2)$ model with a fundamental scalar field. In a high precision simulation of the Higgs phase, masses, α_{ren} and the VOOB were computed at $\lambda = \infty$, $2.4 \leq \beta \leq 3.0$, close to the Higgs-confinement transition, on lattices up to $12^3 \times 24$. At $\beta = 3.0$, the value of α_{bare} is .106, while the values of α_{ren} were found to be between .25 and .30. Nevertheless, the tree-level relation for renormalized quantities:

$$(am_W)^2 = \frac{1}{2} g_{ren}^2 (av)^2 = 2\pi \alpha_{ren}^2 \kappa \rho(\infty, \infty) \quad (18)$$

was fulfilled rather accurately. Becoming bold, we can estimate the value of λ_{ren} using as definition the tree-level relation

$$\lambda_{ren} = \frac{m_H^2}{4v^2} = \frac{(am_H)^2}{4\kappa\rho(\infty, \infty)} \quad (19)$$

Here m_H denotes the mass of the Higgs particle as defined in section 3.1. Again at $\beta = 3.0$, the values obtained in this way for λ_{ren} are not too large ($\lambda_{ren} \leq 3$ for the narrow range $\kappa_{cr} < \kappa \leq .36$ above the transition), although $\lambda_{bare} \equiv \lambda = \infty$. In fact they are smaller than in the pure matter theory ($g = 0$) at $\lambda = \infty$ and at the same values of am_H , as can be seen by comparing with the results of [25,22,23,24]. Thus although both α_{ren} and λ_{ren} differ a lot from their bare values, they are relatively small and there is a chance that the renormalized perturbation theory is a good computational tool. One should however be careful. We are in the neighbourhood of the phase transition. If the Coleman-Weinberg arguments [17] apply, not all relevant properties can be computed using tree level relations. Actually the degree of accuracy to which (18) is fulfilled gets worse as β is lowered; at $\beta = 2.7$ it is still rather well obeyed, but at $\beta = 2.4$ this is no longer the case. Notice that we have found a region where a highly nontrivial check on the validity of perturbation theory can be performed as pointed out at the beginning of section 3. For that, a renormalized perturbative calculation beyond leading order should be performed for the measured quantities and then compared to the Monte Carlo results.

It is interesting to note that $U(1)$ analog of the relation (18) was also fulfilled well, albeit within larger statistical errors, in the simulation [44] that we used in section 3.1 as an example for mass calculations.

The VOOB can be generalized to compute two-point-functions for particles that do not transform trivially under the “unbroken” group. The simplest example, that of the vector bosons in the $SU(2)$ -adjoint model (which are charged under a $U(1)$ subgroup of $SU(2)$), is discussed in [53].

3.4 An Example of a Nonperturbative Effect

In Abelian theories, the electric field operators are gauge invariant. This is no longer true for nonabelian theories. The electric fields are generators of the group multiplication operators [5,3,19] (for every link the classical time-zero U -fields are acted upon from the left or from the right with a group element). Only the group multiplications $\mathcal{E}_{\underline{x},j}(c)$ by an element c of the gauge group center are gauge invariant (left and right multiplications coincide for the center and only for the center). Let us define the *gauge invariant electric flux operator* $\mathcal{F}(\underline{\mathcal{S}}, c)$ as the product of the $\mathcal{E}_{\underline{x},j}(c)$ for the links \underline{x}, j perpendicular to a surface $\underline{\mathcal{S}}$ (technically $\underline{\mathcal{S}}$ is a surface on the dual of the three-dimensional time-zero lattice). This is a multiplicative flux.

In the pure gauge theory $\mathcal{F}(\underline{\mathcal{S}}, c)$ has nontrivial commutation relations with the operator *measuring the magnetic flux* through a surface that intersects the boundary $\partial\underline{\mathcal{S}}$ of $\underline{\mathcal{S}}$ in one point [18]. Thus by acting with a center-electric flux operator on the vacuum, we obtain a state that may contain a *closed tube of center-magnetic flux* at $\partial\underline{\mathcal{S}}$ (with the flux quantum number c). The question of whether the magnetic flux is screened dynamically by vacuum fluctuations can be answered using the vacuum overlap of this state (this is the *'t Hooft loop* [18]). If the vacuum overlap is small (area law), we have an excitation of the vacuum; if it is large (perimeter law), then the vacuum is a “condensate” of center-magnetic flux tubes that screen the extra flux tube we are trying to create.

The situation changes in the presence of a matter field in the fundamental representation. The energy of the state obtained by acting with $\mathcal{F}(\underline{\mathcal{S}}, c)$ on the vacuum is proportional to the *area* of $\underline{\mathcal{S}}$ rather than, as in the case in the pure gauge theory, to its perimeter. Even though the commutation relations between the electric and the magnetic fluxes have not changed, the interpretation as a closed tube of center-magnetic flux is no longer possible. This problem can be overcome [19] using an energy regularization method similar to that described in section 3.3 for charge-anticharge states.

For the energy-regularized candidate of a state with a closed center-magnetic flux tube, we can again use the vacuum overlap as a test of whether the vacuum fluctuations screen the magnetic flux or not. In the Higgs region an interesting phenomenon happens [19]. The vacuum overlap is small – i.e. obeys an area law – for small $\underline{\mathcal{S}}$, while for larger $\underline{\mathcal{S}}$ there is a crossover to an asymptotic perimeter law. Thus small center-magnetic flux tubes are relatively stable excitations, while large ones are not. This is a situation similar to that for the energy regularized charge-anticharge states in the confinement region (see section 3.3).

Unless someone comes up with a completely new idea, there is no way to compute perturbatively the quantities discussed above. Therefore we cannot decide whether the fact that in the Higgs region the small closed lines of center-magnetic flux are excitations is a lattice artifact, or whether it is relevant to continuum physics too (e.g. for the deep inelastic scattering of W 's and Z 's).

4 TOWARDS CONTINUUM PHYSICS

In section 2.1 we briefly discussed how to take the continuum limit in models with more than one parameter in the action. We argued that it is useful to first determine the *lines of constant physics* (LCP's) and then investigate how correlation lengths (or, equivalently, the cutoff) grow along such lines. Let us for the sake of simplicity continue the discussion in terms of a specific model. The obvious candidate is the Higgs region of the $SU(2)$ theory with a fundamental scalar field. The most thorough investigations in the literature are for this model. Following [21] we define an LCP by fixing g_{ren} and the Higgs to W mass ratio m_H/m_W . Other definitions give in general different LCP's. If however scaling is well obeyed, which is expected to be the case in the perturbative region at large correlation lengths, the various definitions almost coincide.

Since the experimental value of the weak coupling g_{ren} is small, many features of the theory can be understood by investigating the $g \rightarrow 0$ limit [29], which is the $O(4)$ -symmetric ϕ^4 model. A natural way to define the LCP's of this pure matter theory is to fix λ_{ren} . Using (19) as a definition for λ_{ren} and assuming that g is small enough so that (18) holds, it follows that in the full theory

$$\lambda_{ren} = g_{ren}^2 \frac{m_H^2}{8 m_W^2} \quad (20)$$

As $g \rightarrow 0$ at a fixed value for am_H , both g_{ren} and am_W become zero, but λ_{ren} is almost constant.

In section 4.1 we shall discuss the perturbative calculation of the LCP's [15,21] in the full model. It will turn out that the correlation lengths are bounded on such lines, unless both g_{ren} and λ_{ren} are zero. This is the well known phenomenon of *triviality*: either the regularization cannot be removed (in our case the lattice spacing cannot become zero), or we have a noninteracting theory. The discussion will just be qualitative, without formulas, since the computations on the lattice do not differ significantly from the standard continuum treatments [14,15].

Next we shall turn to the upper bound on the Higgs mass. Consider a line in the phase diagram obtained by fixing g (another possibility is to fix g_{ren}) and λ . From the properties of the LCP's, we shall see that along such a line the values of λ_{ren} and of m_H/m_W increase with am_H , which in turn increases with κ . At some point am_H becomes of the order 1. Since a^{-1} is the cutoff Λ , this means that in physical units the Higgs mass approaches the cutoff. It becomes meaningless to speak of a Higgs *particle* anymore. We declare this value of m_H to be the g_{ren} - and λ -dependent upper bound (e.g. in units of m_W). The interesting bound is the highest upper bound obtained by varying λ . From the behaviour of the LCP's we shall see that this "upper upper bound" is obtained at $\lambda = \infty$, which is one of the reasons why so many numerical calculations are done at this particular value of λ . The bound now depends only on g_{ren} .

Although renormalized perturbation theory may lead to relations that are accurate up to large values of the bare parameters, e.g. up to $\lambda = \infty$, the computation of the upper bound on m_H requires an inherently nonperturbative piece of information, namely the relation between bare and renormalized quantities at large values of λ . One way to obtain these relations numerically is through computer simulations. In section 4.2 we shall briefly describe some recent Monte Carlo calculations of the upper bound [42,22,23,24], performed both in the full model and in the limiting $O(4)$ -symmetric pure matter theory.

For the pure matter theory on the lattice, Lüscher and Weisz [25] developed an analytical method that leads to similar results and is, at present, even more accurate. They start their calculation in the unbroken phase, at small κ , using a high order expansion in κ (which is a nonperturbative method too). The results are then continued to the phase transition and into the broken phase using the renormalization group equations in both phases, which are matched at the phase transition. We end section 4 by briefly discussing this approach.

4.1 Lines of Constant Physics

Hasenfratz and Hasenfratz [15] ended a lot of speculative discussions about the LCP's (see e.g. [41]) by explicitly computing the relevant quantities in a renormalization group improved perturbative expansion around the Gaussian fixed point $g = \lambda = 0$, $\kappa = \frac{1}{8}$. This method is reliable if both the bare and the renormalized couplings are small enough. We are however also interested in the shape of the LCP's for large values of the bare coupling λ , where conventional perturbation theory cannot be used to determine the dependence of renormalized quantities on the bare parameters (even if λ_{ren} is small).

In order to solve this problem, a different approach was taken by Montvay [21]. Following to some extent the suggestions of Dashen and Neuberger [29] he started from the full pure matter theory and expanded in g^2 alone. The advantage of this approach is that, similarly to the pure gauge theory, this is an asymptotically free expansion. The drawback is that the zeroth order theory is the full ϕ^4 model (however, as will be discussed later, this is the model where the best numerical results are available).

Both approaches lead to similar conclusions about the LCP's, which are summarized in figs. 8 and 9. In fig. 8 the projection in the β - λ plane is shown for some typical LCP's. The arrows point in the direction of increasing correlation lengths. Since there is a two-parameter family of LCP's, it is not possible to visualize all of them at once in this way. Some of the LCP's end in the first order transition surface (see section 2), others end at $\lambda = \infty$. For $g \neq 0$ (in our case equivalent to $g_{ren} \neq 0$) no LCP ends at a point in the phase diagram where correlation lengths diverge. In fig. 9 the one-parameter families of LCP's at fixed g_{ren} are shown. On the left we have the pure matter theory. Here all LCP's end

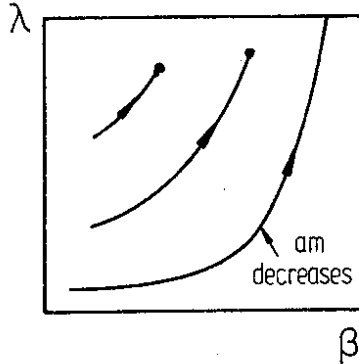


Figure 8: κ -projection of the lines of constant physics (LCP's) in the $SU(2)$ model with a fundamental scalar field (following [21]). The axes extend up to infinity. The arrows point in the direction of increasing correlation lengths (increasing cutoff).

at $\lambda = \infty$ [25]. On the right, at $g_{ren} \neq 0$, the situation is different: the transition line is first order, and there are LCP's that end in it. Notice that λ_{ren} becomes smaller as the LCP's approach the phase transition line. It is zero only in the pure ϕ^4 case, at the transition. This second order phase transition line is also the only LCP along which a correlation length can be infinite.

Let us try to get an intuitive understanding of the shape of the LCP's. Assume we start at a point A in the phase diagram at some sufficiently large β . All correlation lengths are finite here. One of the renormalization group equations contains g alone [14], and is almost identical to that of the pure gauge theory. Since g is asymptotically free, we expect the LCP containing A to move towards smaller values of g as the correlation lengths (equivalently, the cutoff) increase.

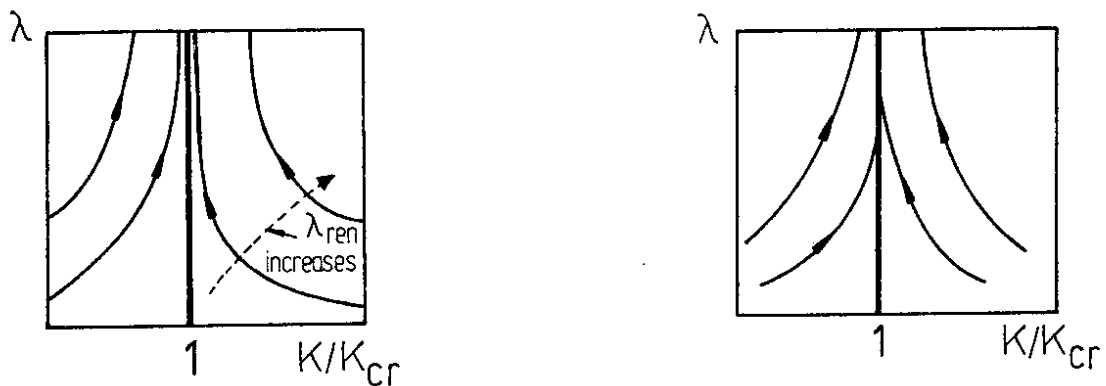


Figure 9: LCP's for a given value of g_{ren} in the $SU(2)$ model with a fundamental scalar field (following [25]); on the left, $g_{ren} = 0$ (pure matter theory), and on the right, $g_{ren} \neq 0$. The axes extend up to infinity. The arrows point in the direction of increasing correlation lengths (cutoff).

On the other hand, if g is small we can as a first approximation neglect it in the renormalization group equation for λ , which is then the same as in the pure matter theory. λ is not asymptotically free, which means that it increases with the correlation lengths (the cutoff). As mentioned above, in the pure matter theory the cutoff is still finite when λ has reached infinity. The non-asymptotically-free coupling has won: the LCP ends before g becomes zero.

Let us sum up. There is no LCP that starts at finite correlation lengths and ends up with at least one of the correlation lengths being infinite. There is one LCP, the phase transition of the pure matter theory, for which the correlation lengths are infinite throughout. On this line however both g_{ren} and λ_{ren} are zero. Thus the continuum limit only exists for a situation in which there is no interaction. This phenomenon is called triviality. If we nevertheless want to use the model for phenomenological purposes, we have to work at a finite cutoff (effective theory). The hope is then that it is the low energy limit of an aesthetically more pleasing theory.

A few words of caution are in place. In the pure matter limit, perturbation theory works well in both phases. If the gauge coupling is turned on, we have at small κ a confinement region instead of a free charge phase. As opposed to the Higgs region, perturbation theory can only be used for a limited set of quantities (short distances). In the discussion of the LCP's at $g \neq 0$ it was important to assume that the Higgs-confinement transition surface is first order. The arguments for that [17] are based on a one-loop study of the effective potential in *both* phases, and are therefore less reliable than the arguments that use the perturbation theory in the Higgs phase alone (see also the remarks in section 2.2).

4.2 Computations of the Upper Bound on the Higgs Particle Mass

In order to obtain the shape of the LCP's, we needed to know the dependence of g_{ren} and m_H/m_W (or, by (20), λ_{ren}) on the bare couplings. For the upper bound on the Higgs mass we also need the dependence of am_H on κ , β and λ .

For $g \neq 0$ the corresponding computation was performed using continuum perturbation theory [14]. As discussed before, this cannot be trusted too much for large bare couplings. At $g = 0$ this problem was circumvented by using an approximate block spin renormalization group method [54], and, on the lattice, by using the method described in the next subsection [25].

Eliminating the bare couplings, one can plot the results for a fixed g_{ren} as shown in fig. 10. The LCP's are here simply horizontal lines. The thick curve contains the upper bounds for $(am_H)^{-1}$, so the region above it cannot be reached. These upper bounds are obtained for $\lambda = \infty$. We have to make a convention for the lowest admissible value of the ratio between the cutoff and the Higgs mass, e.g. $\Lambda/m_H \equiv (am_H)^{-1} > C$, with C a constant larger than but of the order of 1.

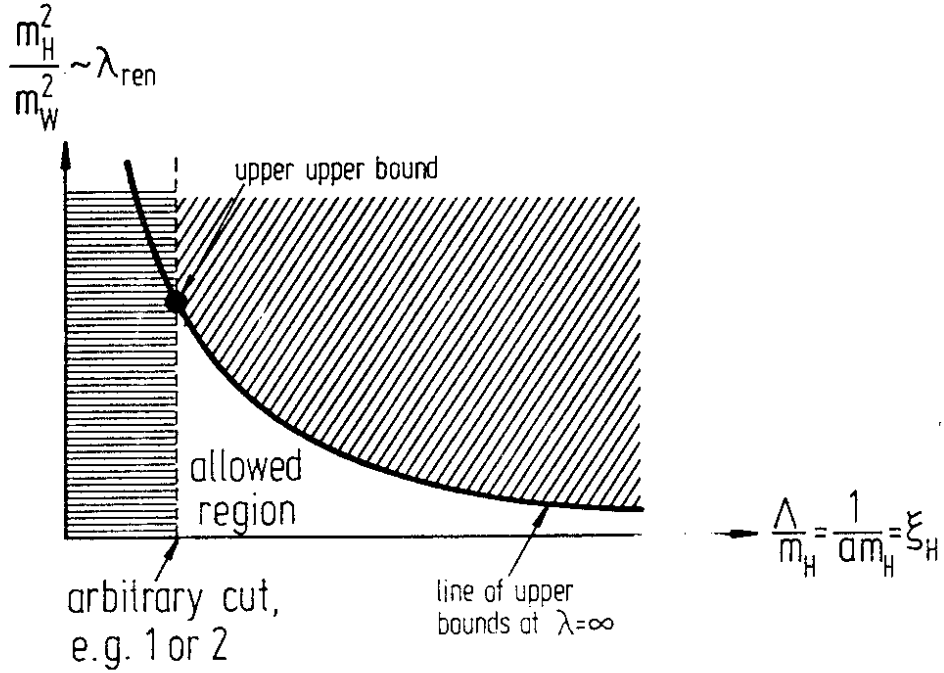


Figure 10: Upper bound for the Higgs mass at fixed g_{ren} . The x-axis is logarithmic.

The region of the x-axis to the left of C is thus also forbidden. The highest upper bound is obtained when the curve of upper bounds reaches C . A change in the definition of C modifies this bound only a little because the x-axis is logarithmic.

It is an important problem to confirm these results by an entirely nonperturbative method. Several computer simulations have been performed to this end.

In [42] the Higgs and the W masses have been measured at a value of g_{ren} close to the experimental one. These calculations have to deal with the problem that at the resulting values of m_H/m_W of around 9, and at $am_H < 1$ (which is required for the bound calculation), the value of am_W is so small that the finite size effects cannot be controlled reliably. Therefore it is more practical to try to find the upper bound on λ_{ren} in the pure matter theory, and use (20), with the experimental values for g_{ren} and m_W to translate it into a value for m_H .

In order to determine λ_{ren} in the pure matter theory, one has to employ (19) and use $v = \langle \phi_{ren} \rangle = MZ^{-\frac{1}{2}}$. Here M is the magnetization and Z is the wave function renormalization corresponding to the Goldstone particles [29].

In [22] m_H and $\langle \phi_{ren} \rangle$ were computed in the pure matter theory. Initially the Z -factor was estimated as the residue at the Higgs resonance pole of a two-point-function used to measure m_H . By comparing the decay of two different two-point-functions that couple to the Higgs, it was later possible to extract the Z -factor for the Goldstone particles too.

There are two calculations that compute the effective potential for the pure matter theory [23,24]. We cannot describe their methods here. In [23] two- and four-point-functions are also measured. Actually the investigations in [23] are more comprehensive: besides the upper bound problem, both phases are considered, scaling laws are checked etc. This is also the simulation with the highest statistical accuracy from the ones mentioned here.

In [24] regularizations of the continuum ϕ^4 theory on lattices of various geometry (not only hypercubic) are considered. The results agree within roughly 10%, which is reassuring, since in the absence of a continuum limit the different regularizations are in fact *different theories*.

The upper bounds obtained in all these calculations agree with one another within statistical errors. They are also consistent with the result quoted in [25] (see below), which is $m_H \leq 630(25)\text{GeV}$ at $\Lambda/m_H=2$. At this value of the upper bound, $\lambda_{ren} = 3.2(2)$, which is small enough for the renormalized perturbation theory to be applicable. This excludes a strongly coupled Higgs sector.

We saw before that there is no interaction if the cutoff becomes infinite. We can however consider a cutoff of the order of the Planck mass. Due to the fact that the x-axis in fig. 10 is logarithmic, the upper bound on the Higgs mass then goes down to about 150 GeV. Such a result certainly cannot be obtained from a direct lattice simulation. However, we can use the simulation results (from lattices of reasonable size) as initial conditions for integrating the renormalization group equations.

4.3 The Lüscher-Weisz Program

Lüscher and Weisz have devised a method to perform very accurate analytical calculations in lattice ϕ^4 models [25].

For small κ there exists a cluster expansion whose convergence can be well controlled and for which relatively high orders can be computed. If one goes to a high enough order, so that all clusters up to a given size r are considered, then the cluster expansion will give very precise results in a region where the correlation length is smaller than r . Realistically, one can go up to correlations of two lattice units.

Fortunately a correlation length of two is already well inside the region next to κ_{cr} where perturbation theory works well. One can use the renormalization group equations to continue the convergent expansion results up to κ_{cr} and then further on into the broken phase. In fig. 11 the solid curve represents the phase transition. In the region *A* the cluster expansion is used. Its results on the dashed line between *A* and *B* are the initial data for solving the renormalization group equations. In order to match the two renormalization group flows at the transition, the massless theory at κ_{cr} was solved. The second dashed line, above *C*, represents

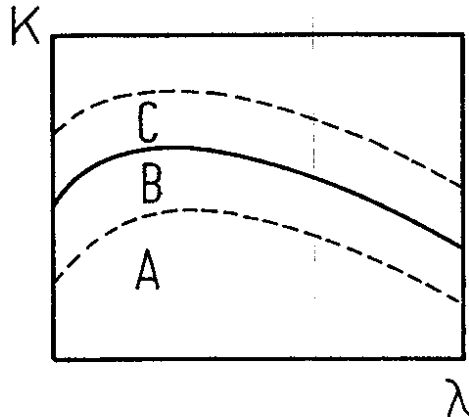


Figure 11: Phase diagram for the pure matter theory (from [25]).

the region above which the solution of these equations corresponds to a correlation length smaller than two. As a consistency check, the solution of the differential equations and of the convergent expansion results are found to be almost identical for a large portion of the region B.

If correct, this analytical method is superior to any other known approximation scheme for the lattice ϕ^4 -theory. There is however no rigorous proof that the renormalization group equations using the perturbative beta-functions are accurate. The main device to test the validity of this approach is a comparison with a completely nonperturbative calculation.

The results of Lüscher and Weisz completely agree with the computer simulations discussed before, and with some very accurate simulations that have been performed with the specific aim of checking them [55].

5 Outlook

In the near future, the investigation of the $SU(2)$ model with fundamental scalars will continue. It is also worthwhile to consider the $U(1)$ case more closely, especially in view of studying the scalar sector of the full standard model.

After having understood the zero temperature properties of these models well enough, a further step is to investigate them at finite temperatures more thoroughly than was the case up to now.

More complicated gauge-Higgs models are of great interest both from the field theoretical, and from the model building point of view.

Last but not least, a lot of effort has gone recently into the study of models with scalars and fermions, in order to investigate what happens at strong Yukawa couplings. This is maybe the area where most work will be done in the near future.

REFERENCES

1. Wilson, K. G., Phys. Rev. D10, 2445 (1974).
2. Osterwalder, K. and Seiler, E., Ann. Phys. (N. Y.) 110, 440 (1978).
3. Seiler, E., "Gauge Theories as a Problem of Constructive Quantum Field Theory and Statistical Mechanics", Lecture Notes in Physics 159, Springer (1982).
4. Drouffe, J. M. and Zuber, J. B., Phys. Rept. 102C, 1 (1983).
5. Creutz, M., "Quarks, Gluons and Lattices", Cambridge University Press (1983); Kogut, J., Rev. Mod. Phys. 51, 659 (1979) and 55, 775 (1983).
6. See e.g. "Field Theory on the Lattice" (Seillac 1987), edited by A. Billoire, R. Lacaze, A. Morel, O. Napoly and J. Zinn-Justin, Nucl. Phys. B (Proc. Suppl.) 4 (1988), part IX.
7. See e.g. the Seillac proceedings (cited above), part III.
8. Wilson, K. et al., in "Lattice Gauge Theory '86" (Brookhaven 1986), edited by H. Satz, I. Harriety and J. Potvin, Plenum (1987), p. 425.
9. Creutz, M., Jacobs, L. and Rebbi, C., Phys. Rept. 95C, 201 (1983).
10. For a review of results obtained before 1986 see:
Jersák, J., in "Lattice Gauge Theory - a Challenge to Large Scale Computing" (Wuppertal 1985), edited by B. Bunk, K. H. Mütter and K. Schilling, Plenum (1986), p. 133.
11. Shrock, R. E., in the Seillac proceedings (cited above), p. 373.
12. Elitzur, S., Phys. Rev. D12, 3978 (1975).
13. See e.g. Abers, E. S. and Lee, B. W., Phys. Rept. 9C, 1 (1973).
14. For a discussion of triviality in the standard model see:
Lindner, M., Z. Phys. C31, 295 (1986);
Lindner, M. and Grzadkowski, B., Phys. Lett. 178B, 81 (1986);
For further references see: Callaway, D. J. E., Rockefeller University preprint RU/87/B1/20, to appear in Phys. Rept.
15. Hasenfratz, A. and Hasenfratz, P., Phys. Rev. D34, 3160 (1986).
16. For a review of "strongly coupled Higgs models" see Gatto, R., Geneva University preprint UGVA-DPT-1986/02-493, published in the proceedings of the 1st Turin Meeting on Superunification and Extra Dimensions (1985).
17. Coleman, S. and Weinberg, E., Phys. Rev. D7, 1888 (1973).
18. 't Hooft, G., Nucl. Phys. B138, 1 (1978), and B153, 141 (1979);
Mack, G. and Petkova, V. B., Ann. Phys. (N. Y.) 123, 442 (1979), and 125, 117 (1980).
19. Fredenhagen, K. and Marcu, M., in the Seillac proceedings (cited above), p. 451.
20. Fredenhagen, K. and Marcu, M., Commun. Math. Phys. 92, 81 (1983), and Phys. Rev. Lett. 56, 223 (1986);
Fredenhagen, K., in "Fundamental Problems of Gauge Field Theories" (Erice 1985, edited by G. Velo and A. S. Wightman, Plenum (1986), p. 265;
M. Marcu, in the Wuppertal proceedings (cited above), p. 267, and in the Brookhaven proceedings (cited above), p. 223.
21. Montvay, I., Nucl. Phys. B293, 479 (1987).

22. Hasenfratz, A., Jansen, K., Lang, C. B., Neuhaus, T. and Yoneyama, H., Phys. Lett. 199B, 531 (1987);
Hasenfratz, A., Jansen, K., Jersák, J., Lang, C. B., Neuhaus, T. and Yoneyama, H., preprint HLRZ Jülich 88-02, UNIGRAZ-UTP-03-88.
23. Kuti, J. and Shen, Y., Phys. Rev. Lett. 60, 85 (1988);
Kuti, J., Lin, L. and Shen, Y., in the Seillac proceedings (cited above), p. 397. Kuti, J., Lin, L. and Shen, Y., San Diego preprint UCSD/PTH 88-05;
Shen, Y., Kuti, J., Lin, L. and Meyer S., San Diego preprint UCSD/PTH 88-06; the last two refs. to appear in the proceedings of the *Lattice Higgs workshop*, Tallahassee (May 1988).
24. Bhanot, G. and Bitar, B., Tallahassee Preprint FSU-SCRI-88-50 and -52, the latter to appear in the proceedings of the *Lattice Higgs workshop*, Tallahassee (May 1988).
25. Lüscher, M. and Weisz, P., Nucl. Phys. B290, 25 (1987), B295, 65 (1988), and DESY preprint 88-083;
Lüscher, M., DESY preprint 87-159, to appear in the proceedings of the Cargèse summer school 1987.
26. Wolff, U., Nucl. Phys. B280, 680 (1987), and Phys. Lett. 207B, 185 (1988).
27. O’Raifeartaigh, L., Rep. Prog. Phys. 42, 159 (1979).
28. See e.g. Montvay, I., Rev. Mod. Phys. 59, 263 (1987).
29. Dashen, R. and Neuberger, H., Phys. Rev. Lett. 50, 1897 (1986).
30. See e.g. Kawai, H., Nakayama, R. and Seo, K., Nucl. Phys. B189, 40 (1981), Reisz, T., Commun. Math. Phys. 116, 81 and 573 (1988), 117, 79 (1988), DESY preprint 87-137, and Max Planck Institute preprint MPI-PAE/PTh-27/88.
31. Brezin, E., Le Gillou, J. C. and Zinn-Justin, J., in *Phase Transitions and Critical Phenomena* Vol. VI, edited by C. Domb and M. S. Green, Academic Press (1976).
32. Fradkin, E. and Shenker, S., Phys. Rev. D19, 3682 (1979).
33. Guth, A., Phys. Rev. D21, 2291 (1980).
34. Evertz, H. G., Jersák, J., Neuhaus, T. and Zerwas, P. M., Nucl. Phys. B251, 279 (1985);
Gupta, R., Novotny, M. A. and Cordery, R., Phys. Lett. 172B, 86 (1986);
Lang, C. B., Phys. Rev. Lett. 57, 1828 (1986), and Nucl. Phys. B280, 255 (1987);
Decker, K., Hasenfratz, A. and Hasenfratz, P., Nucl. Phys. B295, 21 (1988).
35. Creutz, M., Jacobs, L. and Rebbi, C., Phys. Rev. D20, 1915 (1979).
36. Evertz, H. G., PhD thesis, Aachen (1987).
37. Nill, F., PhD thesis, Max-Planck Institute München MPI-PAE/PTh 31/87 (1987), and in preparation.
38. Vilkoviskii, G. A., Nucl. Phys. B234 125 (1984);
De Witt, B. S., in *E. S. Fradkin’s 60th Birthday Volume*, Adam Hilger (1986).
39. Osterwalder, K. and Schrader, R., Commun. Math. Phys. 42, 281 (1975).
40. Evertz, H. G., Jersák, J., Lang, C. B. and Neuhaus, T., Phys. Lett. 171B (1986) 271.
41. Montvay, I., Nucl. Phys. B269, 170 (1986);
Langguth, W., Montvay, I. and Weisz, P., Nucl. Phys. B277, 11 (1986).
42. Langguth, W. and Montvay, I., Z. Phys. C36, 725 (1987);
Hasenfratz, A. and Neuhaus, T., Nucl. Phys. B297, 205 (1988).

43. Katznelson, E., Lauwers, P. and Marcu, M., in the Seillac proceedings (cited above), p. 427;
Evertz, H. G., Katznelson, E., Lauwers, P. and Marcu, M., Bonn University preprint HE-88-13, to appear in the proceedings of the *Lattice Higgs workshop*, Tallahassee (May 1988).
44. Evertz, H. G., Jansen, K., Jersák, J., Lang, C. B. and Neuhaus, T., Nucl. Phys. B285, 590 (1987).
45. Lee, I-H. and Shigemitsu, J., Phys. Lett. 169B, 392 (1986), Nucl. Phys. B276, 580 (1986), and B263, 280 (1986).
46. Brezin, E. and Zinn-Justin, J., Nucl. Phys. B257, 867 (1985).
47. Barata, J. C. A. and Fredenhagen, K., in the Seillac proceedings (cited above), p. 639.
48. Evertz, H. G., Grösch, V., Jersák, J., Kastrup, H. A., Landau, D. P., Neuhaus, T. and Xu, J.-L., Phys. Lett. 175B (1986) 335.
49. Filk, T., Marcu, M. and Fredenhagen, K., Phys. Lett. 169B, 405 (1986).
50. Evertz, H. G., Grösch, V., Jansen, K., Jersák, J. and Kastrup, H. A. and Neuhaus, T., Nucl. Phys. B285 (1987) 559.
51. Azcoiti, V. and Tarancon, A., Phys. Lett. 176B, 153 (1986).
52. Azcoiti, V., Di Carlo, G., Grillo, A. F., Cruz, A. and Tarancon, A., Phys. Lett. 200B, 529 (1988).
53. Fredenhagen, K., Filk, T., Marcu, M. and Szlachanyi, K., to appear as DESY preprint.
54. Hasenfratz, P. and Nager, J., Z. Phys. C37, 477 (1988).
55. Montvay, I. and Weisz, P., Nucl. Phys. B290, 327 (1987);
Montvay, I., Münster, G. and Wolff, U., DESY preprint 88-049.